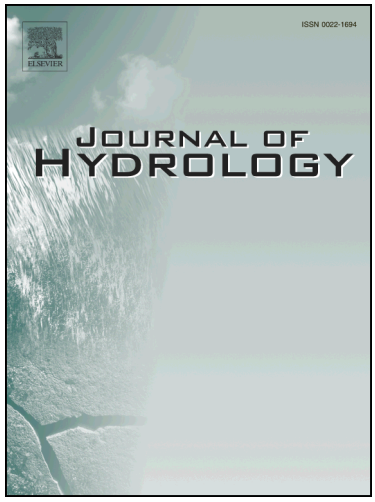

Research papers

Bed-mounted Electro Magnetic meters: Implications for robust velocity measurement in Urban Drainage Systems

Damjan Ivetić, Dušan Prodanović, Luka Stojadinović

PII: S0022-1694(18)30671-1
DOI: https://doi.org/10.1016/j.jhydrol.2018.08.068
Reference: HYDROL 23082

To appear in: *Journal of Hydrology*

Received Date: 3 July 2018
Accepted Date: 28 August 2018

Please cite this article as: Ivetić, D., Prodanović, D., Stojadinović, L., Bed-mounted Electro Magnetic meters: Implications for robust velocity measurement in Urban Drainage Systems, *Journal of Hydrology* (2018), doi: https://doi.org/10.1016/j.jhydrol.2018.08.068

Bed-mounted Electro Magnetic meters: Implications for robust velocity measurement in Urban Drainage Systems

Damjan Ivetić [1], Dušan Prodanović [2], Luka Stojadinović [3]

[1] PhD Student, University of Belgrade, Faculty of Civ. Eng., Bul. kralja Aleksandra 73, Belgrade 11000, Serbia, (corresponding author) e-mail: *divetic@grf.bg.ac.rs*

[2] Professor, University of Belgrade, Faculty of Civ. Eng., Bul. kralja Aleksandra 73, Belgrade 11000, Serbia

[3] MSc Student, University of Belgrade, Faculty of Civ. Eng., Bul. kralja Aleksandra 73, Belgrade 11000, Serbia

ABSTRACT

Flow monitoring in Urban Drainage Systems (UDS) is required for a successful system control and operational assessment. Commonly used methods can lead to erroneous results in partially filled pipes and hostile environmental conditions, normally encountered in UDS. Recent studies focused on the flow rate measurements in UDS revealed that the capability of acoustic Doppler velocimeters to estimate mean flow velocity is impeded by several factors. Most prominent issues are the operation under low flow depths and velocities, as well as in the case of the sedimentation at low flow velocities. This study is focused on an alternative method for the velocity measurements in the UDS, based on Electro-Magnetic Velocity (EMV) meters. The study also determines the sensor's capacity to operate when covered by a porous sediment layer, using a newly developed procedure. A brief theoretical background is given to support the idea behind the usage of EMV in UDS. Measurement uncertainties were firstly benchmarked in the laboratory flume without sediment. After local, site-specific (re)calibration, EMV operated with combined uncertainty of only few cm/s. Furthermore, the EMV measured the flow rates with depths low as 4 cm and velocities bellow 5 cm/s. Additionally, a series of tests were performed with sediment layers above the EMV meter, varying in height from 0 to 80 mm. Observational uncertainty analysis showed that EMV meter can be used even in these conditions. Since the bias uncertainty increased with the rise of the sediment depth, a correction

function model was derived for the transformation of the output signal, reducing the observational uncertainties below 5 cm/s. Subsequently, practical implications of the EMV usage in the UDS are considered.

Keywords:

Velocity measurements, Urban Drainage Systems, Sedimentation, Electro Magnetic Velocity meters, Uncertainty, Laboratory test

List of Abbreviations

UDS	Urban Drainage System
EMV	Electro-Magnetic Velocity (meter)
VA	Velocity – Area
CV	Control Volume
ADV	Acoustic Doppler Velocimeters
EMF	Electro-Magnetic Flow (meter)
EM	Electro-Magnetic
GUM	Guide to the expression of Uncertainty in Measurement
RMSE	Root Mean Square Error
UZ	Unaffected Zone
MA	Model Applicability
OoB	Out of Bounds
CFM	Correction Function Model
SME	Small and Medium Enterprise

List of Symbols

$A(h)$, A	Cross – sectional area [m^2]
E	Induced voltage between the electrodes [V]

$\vec{V}$	Streamwise velocity field [m/s]
$\vec{B}$	Magnetic induction [T]
w	Weight function [/]
$\vec{W}$	Weight vector [/]
$\vec{j}$	Virtual current vector [A/m^2]
τ	Control volume [m^3]
L	Sensor length
W	Sensor width
H	Sensor height
δ	Sediment depth
Q	Flow rate [m^3/s]
Q_{EMF}	Flow rate measured with the referent EMF meter [m^3/s]
V_B	Benchmark mean velocity, EMF velocity [m/s]
h	Water depth [m]
j	Trial number in experiments without sediment cover
$h_{b,j}$	Benchmark water depth measurement in j-th trial [m]
i	Observation number
$V_{EMV,i,j}$	Velocity measurement i in the j-th trial [m]
n	Number of i observations in each trial j
N	Number of trials in the experiment without sediment cover
$\overline{V_{EMV,J}}$	Mean of the i velocity measurements in trial j [m/s]
$S_{EMV,j}$	Standard deviation of the i velocity measurements in trial j [m/s]
$\overline{V_{B,J}}$	Mean of the i benchmark velocity measurements in trial j [m/s]
$u(V)_b$, $u(V)_{b,adj}$	Bias, adjusted bias uncertainty [m/s]
$u(V)_P$	Precision uncertainty [m/s]

$u(V)_B$	Benchmark uncertainty [m/s]
$u(V)_c$	Combined uncertainty [m/s]
W	Flume width [m]
Fr	Froude number
$\overline{V_{EMVadJ,J}}$	Adjusted mean of the i velocity measurements in trial j [m/s]
URF_x	Uncertainty Reduction Factor
$u(V)_{x,ADV}$	Uncertainty of the ADV velocity measurements [m/s]
$u(V)_{x,EMV}$	Uncertainty of the EMV velocity measurements [m/s]
C_u	Uniformity coefficient
C_c	Coefficient of curvature
D_{10}, D_{50}, D_{90}	Diameter at which 10%, 50% or 90% respectively, of the sample's mass is comprised of particles with a diameter less than this value.
k	Trial number in experiments with sediment cover
N_{sed}	Number of trials in the experiments with sediment cover
m	Experiment run number in the experiments with sediment cover
M	Number of experiment runs in the experiments with sediment cover
$\overline{V_{EMV,k,m}}$	Mean of the i velocity measurements in trial k for the m-th experiment run [m/s]
$\overline{V_{B,k,m}}$	Mean of the i benchmark velocity measurements in trial k for the m-th experiment run [m/s]
δ_m	Sediment depth in the m-th experiment run [m]
$\alpha_m, \alpha_{m,mod}$	Correction function slope and modelled correction function slope, respectively, for the m-th experiment run [/]
$\beta_m, \beta_{m,mod}$	Correction function intercept and modelled correction function intercept, respectively, for the m-th experiment run [/]
f_m	Linear correction function for the m-th experiment run
f_{amp}	Correction function slope (amplification) meta-model

f_{zero} Correction function intercept (zero-drift) meta-model

1. INTRODUCTION

The increase of the public environmental awareness is one of the key drivers in the improvement of the knowledge regarding urban drainage and sewer system behavior. Accurate field observations and measurements, such as of flows in Urban Drainage Systems (UDS), are essential for estimating pollutant loads and better understanding of impacts on the urban aquatic environment. The importance of flow measurements for the UDS management was first recognized in the 1970s when basic flood gaging stations were introduced in and upstream of urban areas (Owen, 1979). Due to the escalating water quality management issues within the stormwater paradigm, flow measurements have gained further prominence (Roy et al., 2008). Additionally, the complexity of design and operation of UDS has increased over time, along with the user expectations and the number of constraints needed to be accounted for (Bertrand-Krajewski et al., 2003; Prodanović, 2008). Furthermore, the requirement for continuous flow monitoring increased when real-time flow control was identified as one of the key approaches for successful UDS management (Schutze, 2002; Roy et al., 2008). Therefore, to provide reliable and continuous flow data, the selection and maintenance of a measuring equipment must meet more stringent requirements (WERF, 2002; Schutze et al., 2004).

Flow measurements in UDS present a challenging task, as the systems are designed to operate with partially filled pipes commonly characterized by hostile environmental conditions. The choice of the optimal measuring method is governed by hydraulic, physical and environmental conditions along with the properties of the flowing fluid (Godley, 2002). The Velocity-Area (VA) methods are most frequently used in UDS. Although the VA methods have higher uncertainty (5 – 10%) in flow rate estimations than those reported for weirs, gates, and flumes (2 – 5%, Campisano et al., 2013), it is more applicable due to hydraulic conditions in sewers. In the VA method, flow data is acquired through a combination of continuous water level and velocity measurements. Water level measurements (h) are used to obtain the wet cross-sectional area, via the calculated $A(h)$ relation,

while the measured velocity must be corrected to obtain the mean flow velocity. Maheepala et al. (2001), Bonakdari and Zinatizadeh (2011) and Aguilar et al. (2016) have shown that the main contribution to the flow rate measurement uncertainty is emanating from the mean velocity assessment.

Typically, a bed-mounted acoustic Doppler velocimeters (ADV) are used for the continuous flow monitoring in UDS (Larrarte et al., 2008). They measure one-dimensional velocity or, less frequently, a velocity profile. ADVs are easy to install, versatile and have a low environmental impact (McIntyre & Marshall, 2008). However, it was shown that their ability to provide accurate measurement of velocity in UDS is impeded by several factors (Maheepala et al., 2001; McIntyre & Marshall, 2008; Aguilar et al., 2016). One of the issues is related to the positioning of the ADV sensor on the pipe bottom, exposing the sensor to sedimentation at low flow velocities and debris accumulation during storm events. The situation can potentially lead to errors or data loss when velocity transducer is blocked or excessive turbulence is created – hence, frequent maintenance interventions are needed. Furthermore, the performance of the ADV method is poor for low flow depths and/or with low flow velocities, making the monitoring of low flow rates erroneous. Additional problems (e.g. related to the uneven vertical distribution of sediment) were reported by McIntyre & Marshall (2008), Nord et al. (2014) and Aguilar and Dymond (2014). To overcome the issue of missing flow data, Maheepala et al., (2001) recommended using additional low-cost depth measuring equipment. However, more reliable velocity measurement alternatives are still needed.

One of the alternatives, or a supplement to the ADV could be the Electro Magnetic (EM) velocity sensing technology. Generally, EM velocity sensing technology requires a flow of a conductive fluid (e.g. water) and is governed by the Faraday's law of induction (Shercliff, 1962). EM flow (EMF) meters are widely adopted for the pressurized flows, being established as robust and accurate - for axisymmetric flows errors lower than 0.1% have been reported (Leeungculsatien & Lucas, 2013) and 0.2-0.5% are standard. However, bed-mounted Electro Magnetic Velocity (EMV) meters are not commonly used for the velocity assessment in the UDS. Inherently, due to its operating principle, EMVs are more robust and reliable when compared to the ADVs and could provide stable and linear

one-dimensional (or two-dimensional) measurements of the flow velocity. Design constraints limit the reach of the EMV's control volume (CV) to the relative vicinity of the sensor, making the velocity measurements more "local" in comparison to the ADV. On the other hand, as the generated magnetic field is unaffected by the sediment concentrations, EMV has a potential for operation under sediment cover, a condition commonly causing flow rate data gaps in the UDS.

The "measurement" or "observation" uncertainty (McMillan et al., 2012) associated with the sensor observations, and defined in accordance to the *Guide to the expression of Uncertainty in Measurement* (GUM) (JCGM, 2008), provides a metric for the quantification of the sensor's capabilities. As the mean velocity and flow benchmarks are generally not available in the field, the measurement uncertainty needs to be determined in the laboratory conditions. Maheepala et al. (2001) performed flume calibration of ADV sensors that were later placed in the storm sewer pipes. Heiner and Vermeyen (2013) analysed nine sensors in rectangular, circular and trapezoidal channels, including one EMV, but with a rather limited number of flow rate values. Aguilar et al. (2016) defined the laboratory benchmarking procedure for the evaluation of the flow/velocity measurement uncertainty and examined two ADV sensors. While these laboratory investigations provided further insight into the uncertainties of the velocity/flow observations in the UDS, none of them has investigated the prospect of the EMV meter usage in a detailed manner.

Results of the velocity sensor operation under sediment cover are rarely addressed in the literature, although field experience has shown that sediment deposition can lead to the occurrence of data gaps. Basic ADV and EMV operation comparison under the sediment layer was reported in Prodanovic et al. (2012), showing the total signal loss of the ADV with small sediment deposits and appearance of the significant bias on the EMV with larger sediment depths. Nord et al., (2014), examined the effect of the sediment-loaded flow on the observation uncertainty of the bed-mounted ADVs, but without results regarding the possibility of sensor's operation under the layer of the sediment or a debris. Aguilar et al. (2016) also analyzed ADV operation with the upstream plywood debris model, but the impact of the debris sedimentation over the sensor was not analyzed. Due to the working principle of the EMV devices, they are expected to operate under sediment cover, but appropriate laboratory and

field investigations are missing from the literature. Furthermore, there is a need for a benchmarking procedure that would quantify the capacity of the sensor to operate under sediment deposit. Apart from providing insight into the associated measurement uncertainties, such procedure needs to define a methodology for velocity measurement correction for known depth of the sediment layer.

The main focus of this paper is to provide a thorough laboratory investigation of the bottom-mounted EMV meter, normally used in combined foul and storm water sewers. The experiments were designed to test the EMV's ability to operate both in standard conditions and with the presence of porous sediment cover over the sensor. The framework given by Aguilar et al. (2016) for benchmarking measurement uncertainties was used for the analysis of the EMV performance under standard conditions, allowing unbiased comparison between the ADV and the EMV meter. The ability of the EMV to operate under porous sediment cover was investigated in the well-controlled laboratory setup. The river sand was used as Butler et al. (2003) states that most of the sediments found in the storm sewers (and less in the combined sewers) are mainly inorganic and non-cohesive. Based on the experimental investigation and uncertainty benchmarking, a newly developed Correction Function Model (CFM) is proposed. The CFM allows the quantification of the systematic impacts of the examined sediment cover on the uncertainty of the mean velocity assessment and the derivation of the appropriate correction functions for uncertainty reduction. The overall aim of the research is to support the effort for the accurate and continuous flow measurement in the UDS, with less frequent data gaps, hence providing an additional value in the pollution load management and real-time control of the UDS.

The paper has been structured in the following manner: firstly, in the methodology section the brief overview of the EMV theory is presented, supplemented by the summary of the bed mounted flat EMV characteristics. Then the details of the used experimental setups are presented together with the description of the corresponding experimental procedures. Finally, the methodology section is closed with the concept of the procedure for benchmarking mean velocity measurement uncertainty, and the novel procedure for the assessment of the capacity of the EMV sensor to operate under sediment cover. Results of the uncertainty analysis of EMV operation in standard conditions are presented and

compared with the ADV. Subsequently the results of the novel procedure for benchmarking EMV's capacity to operate under sediment cover are shown. Practical implications of the laboratory findings are discussed and the directions for future research are defined.

2. METHODOLOGY

2. 1. Mean velocity measurement with the EMV meter

Mean velocity estimation, needed for the VA flow measurement method, is in general troublesome task that requires special care and knowledge (Bonakdari and Zinatizadeh, 2011). The EMV meters are rarely employed in UDS for this purpose, thus the basics of the EM velocity sensing technology are given in the following subsection. Subsequently, the characteristics of the used flat EMV meter are reported, highlighting the benefits of this technology for the velocity measurements in the UDS.

2.1.1. Basics of the EM velocity sensing theory

The review, recently given by Watral et al. (2015), had provided a historical and chronological overview of the most notable research regarding the EM flow/velocity sensing technology. In general, EMV operating principle is based on the Faraday's law of induction, where the output signal of the meter (induced voltage between the electrodes E) is generated by the motion of the conductive fluid through a transversal magnetic field (Shercliff, 1962). To allow for the stationary analysis of the electromagnetic induction phenomenon, typically some electric and magnetic properties of the environment are assumed (Michalski et al., 2001). Originally, under these assumptions, Kolin (1939) has given the basic relationship for the EM theory:

$$\nabla^2 E = \mathrm{div}\left(\vec{V} \times \vec{B}\right) \quad (1)$$

where $\vec{V}$ is the streamwise velocity field, $\vec{B}$ is the magnetic induction and $\mathrm{div}\left(\vec{V} \times \vec{B}\right)$ is treated as a charge distribution. Based on this theory, general sensitivity was described as the cross product of the velocity and the magnetic field at a certain position (Bevir, 1970; Bevir et al., 1981). Furthermore, the relations used in the electrical networks, motivated an idea to describe how each part of the flow contributes to the voltage E through the weight function w (Shercliff, 1962) or in a more rigorous formulation, through the weight vector $\vec{W}$ (Bevir, 1970):

$$E = \int_{\tau} \left(\vec{B} \times \vec{j}\right) \cdot \vec{V} d\tau = \int_{\tau} \vec{W} \cdot \vec{V} d\tau \quad (2)$$

where the cross product $\vec{B} \times \vec{j}$ defines Bevir's weight vector $\vec{W}$, τ is the control volume of the EM sensor (**Fig. 1**) and $\vec{j}$ is the virtual current vector (i.e. the current density set up in the liquid by driving an imaginary unit current between a pair of electrodes).

EMF and EMV meters can be distinguished through the characteristics of the control volume τ (**Fig. 1**). In the bed-mounted EMV application, τ is a variable, dependent on several factors: excitation current, coil design, distribution of the $\vec{B}$, conduits geometry and water depth (for low depths). Since the excitation coil of the bed-mounted EMV sensors is relatively small, the reach of the produced magnetic field is limited to the relative vicinity of the EMV. Thus, bed mounted EMV meters are semi-integrative devices, according to the classification of Steinbock et al. (2016), as usually only parts of cross sectional flow contributes to the output signal (**Fig. 1**).

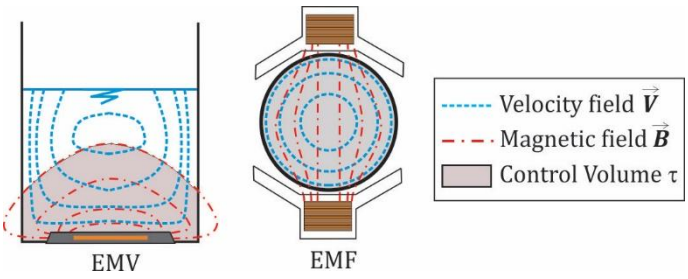

Fig. 1. Cross-sectional illustration of the EMV vs EMF meter application and the reach of the respective control volumes

2.1.2. Bed-mounted flat EMV meter

Throughout the history, different designs of the EMF and EMV meters for free surface flow applications were introduced (e.g. Gils, 1970, Michalski, 2002, Watral et al., 2015). The extensive research given by Herschy & Newman (1974) and Herschy (1978), gave a momentum in a direction of flat coils design, although for purely economic and practical reasons. In the research presented in this paper, bed mounted Flat (coil) DC-2 EMV sensor was used. It is designed by a local SME (Svet instrumenata, 2018) for one-dimensional velocity measurements. The sensors are installed in the appropriate UDS drains, either on the bottom or on the wall (when multiple sensors are used). For minor conduits, smaller Compact Flat DC-2 EMV can be used which operates on the same principle.

Used flat EMV sensor is shaped to minimize the flow disturbances. Two flat excitation coils are integrated into the robust inox housing, with the dimensions of L = 280 mm, W = 160 mm and H = 23 mm (**Fig. 2**). The sensor is connected to external data logger and power source. Data can be collected either wirelessly via GPRS or with the standard RS-232 serial communication. The overall cost of one flat DC-2 EMV unit is below 5000 $, being in a similar price range as the one-dimensional non-profiling ADV. The manufacturer specifies that the accuracy of the DC-2 EMV device is $\pm$1%, precision 0.001 m/s, and the operating range is bidirectional, $\pm$ 15 m/s. The broad operating range and bidirectional operation of the EMVs could be a valuable asset in the combined sewer systems, where the dramatic difference is observed between dry and wet weather flow (Harremoës et al., 1993) combined with possible backwater flow. Factory calibration of each EMV meter is performed in a towing tank simulating nearly homogenous velocity profile. The induced voltage shows a linear relationship with the measured velocity. The power consumption is user controllable: larger coil currents and longer measurement periods will increase the needed power but will lead to better signal/noise ratio. In this research the 10 s measurement interval was used for a single measurement

with coil excitation of 80 mA, while for the rest of the sampling interval the overall consumption is less than 1 mA. Thus, depending on the sensor settings, the power consumption can be even lower than for the ADVs (Aguilar et al., 2016). DC-2 EMV has a pulsed bipolar dual frequency excitation, with the main commutative frequency of 12.5 Hz, providing good noise properties and zero stability (Kuromori et al., 1994). To reduce the effect of conductivity variations on the velocity measurements, the internal resistance of the DC-2 EMV is in the order of 20 MΩ. Therefore, it is estimated that for the worst-case scenario it will be at least 1000 times higher than the resistance of water.

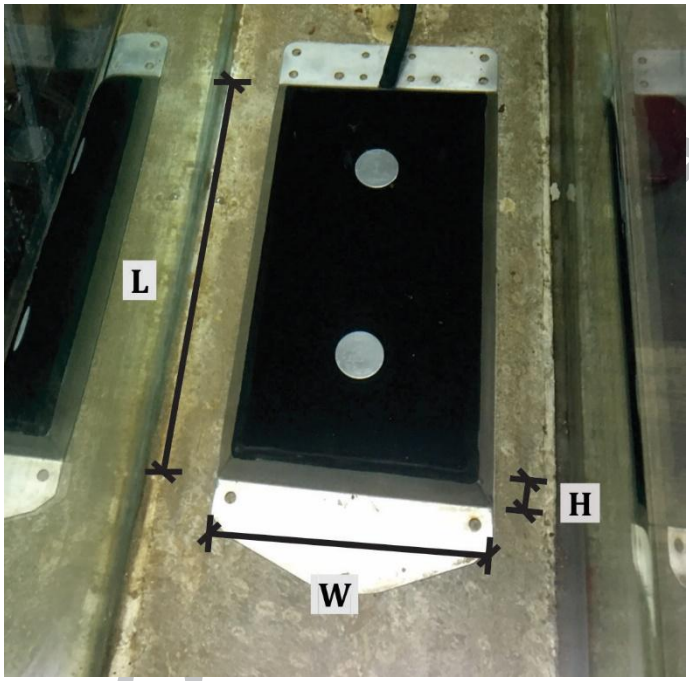

Fig. 2. The Flat DC-2 EMV in the lab flume

The most interesting benefit of the EMV usage in the UDS, which is experimentally examined in this paper, is the possibility of a sensor to operate with the debris sedimentation over the sensor housing. In such conditions, EMV will continue to operate but it will be biased by the presence of the sedimented material. **Fig. 3** presents an illustration of the EMV operation under sediment cover. Since the sediment cover in the UDSs is porous, flowing fluid will be in contact with the electrodes of the sensor allowing for the generation of the voltage E proportional to the flow velocity. On the other

hand, due to the exclusion of the certain zones of the control volume τ which is now occupied by this sediment deposit (where velocities are negligible), the induced voltage E will be smaller. It can be assumed that the reduction of E is proportional to the rise of the sediment depth δ since the fluid flow is moved further away from the EMV's electrodes and the excitation coils, where the magnitudes of the virtual current $\vec{j}$ and the generated magnetic field $\vec{B}$ are smaller. In the investigation presented here, an attempt is made to quantify this systematic effect and to suggest the corrections of the output signal. Using these corrections, the accuracy of the velocity measurements can be maintained even under sediment cover of known depth.

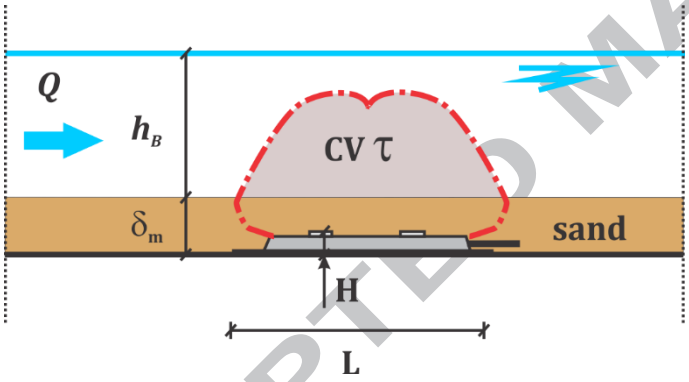

Fig. 3. Illustration of the EMV operation under the sand sediment of depth δ_m

2.2. Experimental setup

To explain the specifics of the experimental setups this section is divided into two subsections: 2.2.1. describes the basic laboratory setup used for the benchmarking velocity measurement uncertainty of the EMV meter in standard (without sediment cover) experiments, and 2.2.2. where the additional details regarding the experiments with the sediment cover are presented.

2.2.1. Basic EMV meter operation in the lab flume

A part of the lab flume in the Faculty of Civil Engineering, University of Belgrade (Serbia), has been adapted for the benchmarking experiments. It accommodates the free surface flow in an 8 m long and 0.25 m wide rectangular channel with a controllable downstream flap gate (**Fig. 4**). The slope of the channel bottom was kept constant at 0.01 %, while the effective Manning roughness is estimated to vary around 0.010 $m^{-1/3}s$. The flume is connected to the variable frequency drive pump, providing flow rates up to 40 L/s and water depths up to 0.4 m. The whole system can also be controlled with a flow control valve placed at the inlet of the flume. At the inlet pipe, a KROHNE Aquaflux F/6 EMF is mounted with an assessed flow measurement uncertainty of 0.6% for extended flow range of 2 L/s - 212 L/s. Depth gauge placed perpendicular to the water level and above the EMV meter, covered the range of depths between zero and 40 cm (h_B), with a benchmark uncertainty of $u(V)_B$ = 0.2 cm. Since the presented system is closed, the conductivity of the water can be considered uniform and constant.

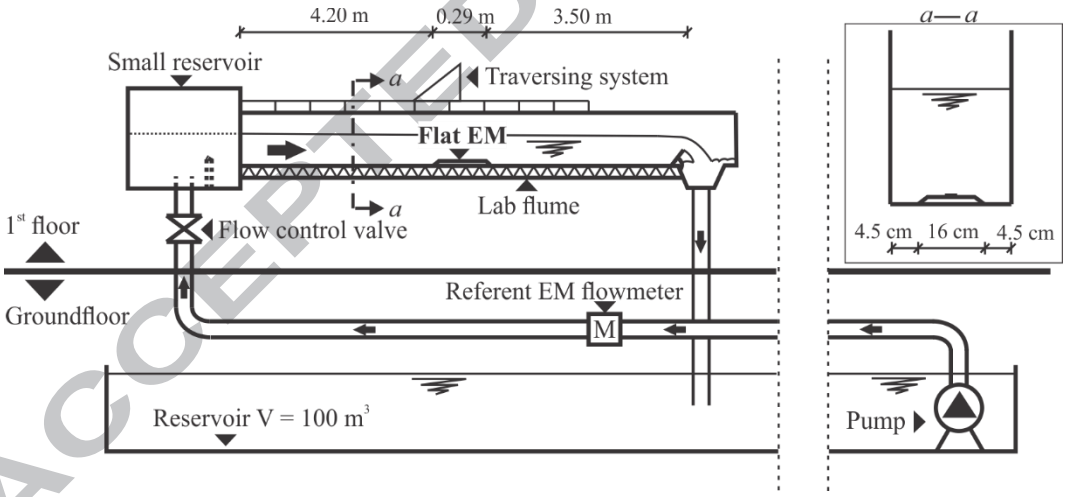

Fig. 4. A schematic illustration of the laboratory flume basic setup as part of the closed circulation system

During the experiments, the flat EMV sensor was positioned and installed 4.5 cm from the vertical channel walls, 4.20 m from the inlet (Small reservoir) and 3.50 m from the outlet (Downstream flap gate). Thus, manufacturer's specifications were satisfied, in terms of the probe orientation and straight

channel run (>10 times the width of the channel). The logger was powered by constant 12V supply. Data was recorded via RS-232 serial port on the laptop PC.

Presented experimental setup is referred to as the "basic setup", which was used for benchmarking velocity measurement uncertainty components in the experiments without sediment cover.

2.2.2. EMV meter operation under porous sediment cover in the lab flume

Experiments with EMV meter covered by controlled layer of sediment required further adaptation of the basic setup **(Fig. 5.)**. The length of the test zone, accommodating sediment presence, was 4.5 m while the width was 0.25 m. The river sand sediment was used, with a relatively uniform grain-size distribution (C_u= 3.57, C_c= 1.12, D_{10}= 0.15 mm, D_{50}= 0.48 mm, D_{90}= 2.30 mm). Although the composition of the river sand used in the experiments does not match the sediment encountered in real UDS, they share the similar non-cohesive and inorganic properties, except in the case of the permanent, undisturbed, and cementitious sediments (Butler et al, 2003). Thus, the river sand might be used to provide the experimental insight into the sensor capabilities in general, which should be verified for the practical purpose with each site-specific sediment. Total of $m = 1 \rightarrow M$ experiments were conducted, with $M = 16$ and the δ_m being defined as the sediment depth in the flume (according to **Fig. 3**). The used sediment depths were $\delta_m = \{0, 5, 10, 15, 20, 23, 25, 30, 35, 40, 45, 50, 55, 60, 65, 70, 80$ mm$\}$. **Fig 6. A** shows the experimental setup for δ_m = 23 mm, corresponding to the height H of the EMV, while **Fig 6. C** setup for the highest examined sediment depth δ_m = 80 mm. Sediment thickness δ_m was measured with several transparent plastic meters placed along the both sides of the flume (distance between two meters ~1.3 m). Depth δ_m was controlled with the acoustic *distance check* function of the Vectrino (Nortek, 2009), mounted on a traversing system **(Fig. 5.)**. Overall uncertainty of the δ_m measurement, with the presented procedure, was adopted to be $\pm$ 1 mm.

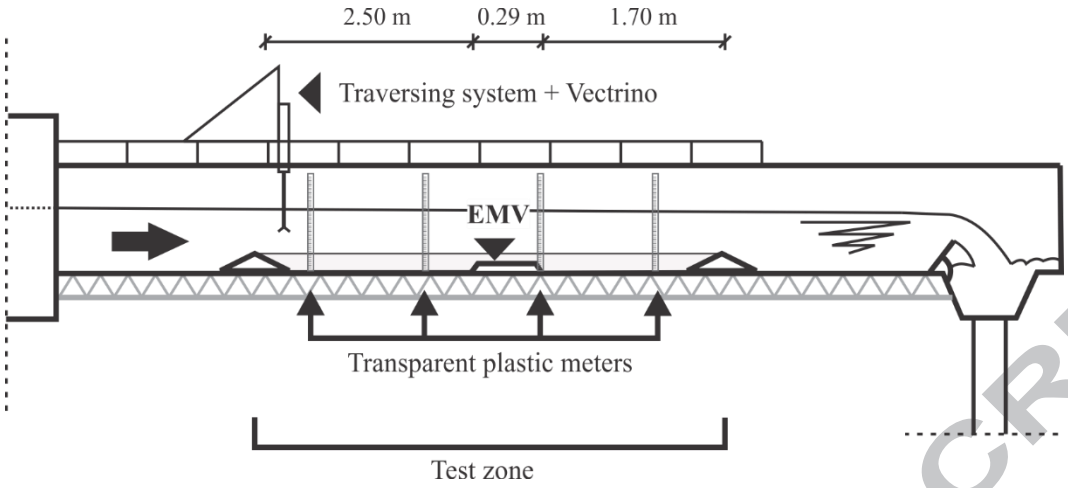

Fig. 5. A schematic illustration of the of the adapted laboratory flume setup for the investigation of the EMV operation under porous sediment cover

The adapted basic setup is referred to as the "sediment setup" and it was used for the assessment of the EMV meter capacity for velocity measurements under porous sediment cover.

2.3. Experimental procedure

For both the basic setup and sediment setup the initial water depth in channel was reached for the zero-flow conditions and flow rate was adjusted with the pump's frequency and using the flow control valve. The EMF was used to provide the benchmark (reference) flow rate value, annotated as Q_{EMF}. As the focus of the investigation was on the mean velocity measurements, the benchmark mean velocity V_B (EMF Velocity) was calculated from the Q_{EMF}, measured depth h_B and known $A(h_B)$ relationship:

$$V_B = \frac{Q_{EMF}}{A(h_B)} \tag{3}$$

2.3.1. Basic EMV meter operation in the lab flume

Prior to the measurements on the basic setup, steady-state conditions were reached for each flow rate. After reaching steady-state conditions, they were maintained for a period of at least 2 min – referred to as "trial" and annotated as j. Depth $h_{b,j}$ was recorded for each trial, and every 30 s velocity observation i was taken by the EMV meter - $V_{EMV,i,j}$. Meanwhile, the EMF flow rate was sampled with 1 Hz frequency and averaged, providing a value $Q_{EMF,i,j}$. The number of observations i for each trial j, was n = 4. Although Maheepala et al. (2001) recommended the 2 min intervals for the flow sampling and Aguilar et al. (2016) used 1 min interval, the 30 s time interval was chosen since the used EMV has excellent signal stability and it was assumed that the practitioners will prefer shorter intervals especially during storm events.

The statistical analysis was performed for each trial, such that i were aggregated into j trials for j = $1 \rightarrow N$ trials. The mean and standard deviation of sensor velocity observations i in trial j were computed and termed as $\overline{V_{EMV,j}}$ and $S_{EMV,j}$, respectively. Similarly, the mean EMF velocity i in trial j (or l) was calculated (eq. 3) and annotated as $\overline{V_{B,J}}$.

The experiments without the sediment cover were used to "locally calibrate" (or, to recalibrate) the flat EMV for the next phase of the investigation (i.e., with sediment cover). The local (re)calibration was needed as the sensor was not operating in the same geometry and flow conditions since the effective size of the control volume τ and velocity distribution were not same as during the factory calibration in a towing tank. To check the actual control volume, the EMV magnetic field $\vec{B}$ mapping was performed (**Fig. 1**). It was concluded that the flume width was insufficient to accommodate the whole control volume τ, hence the effective control volume τ was smaller in the lab experiments than during the factory calibration. Nevertheless, it will be shown that the linearity of the EMV allowed for the effective reduction of this bias with the linear correction function.

2.3.2. EMV meter operation under porous sediment cover in the lab flume

In sediment setup, the $M = 16$ different sediment depths were used. Experiments were run with a decreasing depth of the sand sediment layer. Sand sediment was not artificially compacted, only the top surface of the sediment deposit was flattened to achieve uniform sediment thickness δ_m across the test zone. After verifying the uniform sediment distribution, measurements were collected following the procedure similar to the one described in the section 2.3.1.

For the sake of brevity, trials were annotated with k, although the same number $n = 4$ of observations i was used. The corresponding statistical analysis was performed on each trial k for $k = 1 \rightarrow N_{sed}$ trials, where N_{sed} was between 20 and 30. N_{sed} trials were recorded for each examined sediment depth δ_m. The mean of the i locally calibrated sensor velocity observations, in trial k, for sediment depth δ_m, was annotated as $\overline{V_{EMV,k,m}}$. The analogous referent velocity, obtained with the EMF and depth gauge, was termed $\overline{V_{B,k,m}}$.

Since the focus of the analysis was on the effect of the static sediment cover, the maximum flow velocity was limited to 0.30 m/s to prevent the motion of the smaller fractions and formation of the bed dunes. Apart from a change in the hydraulic properties of the channel (Banasiak, 2008), these bed dunes were causing uncontrollable temporal and longitudinal variation of δ_m. Due to resulting recirculation behind the dune's crests the observed velocity lost the linearity property and these results were excluded from the analysis (**Fig. 6 B**). Thorough and separate investigation is needed to further analyze this phenomenon, which is out of the scope of this paper.

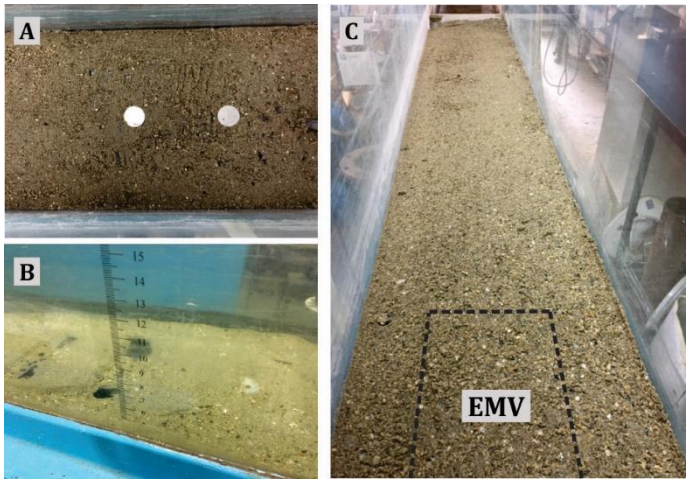

Fig. 6. Experimental setups for the EMV velocity measurements under the sand sediment A) δ_m = 23 mm B) δ_m = 23 mm, dune formation C) δ_m = 80 mm (position of the EMV sensor marked with dashed line)

2.4. Methodology for the assessment of the measured data

The following sections describe the methodology used for the assessment of the acquired velocity data. Aguilar et al. (2016) firstly proposed the procedure for benchmarking measurement bias, precision uncertainty and the computation of the uncertainty of the benchmark itself. Slightly modified procedure was used here, allowing for an unbiased comparison between the ADV and the EMV technology. The comparison was performed through the uncertainty reduction factor, for the velocity measurements made on the basic experimental setup. The uncertainty benchmarking procedure was also applied on the measurements made on the sediment setup with different sediment depths. A novel procedure is proposed for benchmarking EMV meter's capacity to operate under porous sediment cover, based on the results of the uncertainty analysis.

2.4.1. Uncertainty evaluation

The performance of the Bed-mounted EMV meter was quantified using the measurement uncertainty parameter, as suggested by the GUM (JCGM, 2008). Historically, the measurands (the measured values) were usually attributed with the "error" values, described as the difference between the true value and the measurand. Since the true values are almost never known (Moffat, 1988), it was questioned how the "error" term can be operationally helpful. Thus, the "uncertainty" was introduced as "a parameter associated with the result of a measurement that characterizes the dispersion of values that could be reasonably attributed to the measurement" (JCGM, 2008). Coleman and Steele (1995) defined the two components of the observation uncertainty, which Bertrand-Krajewsky and Muste (2008) have applied to the hydrologic measurements: (1) bias uncertainty $u(V)_b$ and (2) precision uncertainty $u(V)_P$ (**Fig. 7**).

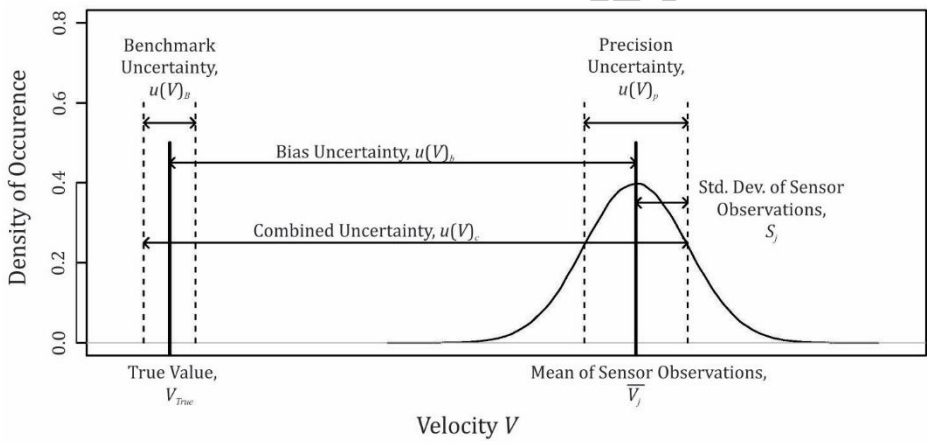

Fig. 7. Uncertainty components and combined uncertainty attributed to the observation of a velocity V, adapted from Coleman and Steele (1995) and Aguilar et al. (2016).

In addition to these uncertainty components, the so-called benchmark uncertainty $u(V)_B$ must be evaluated as it provides the measure of the extent to which the mean velocity can be measured for the particular laboratory installation. The guidelines for the definition of these uncertainty components are presented in Aguilar et al. (2016). Here, the basic characteristics are briefly described, underlining the improvements implemented in the presented benchmarking procedure.

2.4.1.1. Benchmark uncertainty

The benchmark uncertainty $u(V)_B$ in general is also referred to as the epistemic uncertainty – the limit to what can be known about a system; its counterpart is the aleatory (statistical, irreducible or "natural") uncertainty (Merz and Thieken, 2005). In the conditions commonly found in the UDS, the mean flow velocity cannot be directly measured. It is, therefore, not possible to evaluate benchmark uncertainty for this parameter in the field. However, the well-controlled laboratory experiments can provide this value, but it must be categorized as the upper limit of what can be directly measured in the field. Therefore, it is assumed that the instruments used for measurement of the mean flow velocity in the field are at least uncertain as those used in the laboratory.

In the work presented in this paper, the EMF located on the inlet of the lab flume in combination with the depth gauge were used to compute the benchmark value of the mean flow velocity (Eq. **3**). The benefits of the EMF technology, in terms of the low uncertainty of the flow rate measurements in the pressurized flow application, can be exploited if: 1) the EMF is installed according to the manufacturer's recommendations (e.g., in terms of the straight inlet/outlet run), and 2) the EMF is regularly calibrated (ISO9104, 1991). The EMF provides the accurate flow rate data along the wide range of flow conditions in the flume, including those with the value of Froude number close to 1. For given setups and used range of flow rates, the value of the observed uncertainty associated with the flow rate data was 0.6%.

The benchmark velocity $V_{B,i,j}$ was estimated based on the observation of the $Q_{EMF,i,j}$ divided by the cross-sectional flow area, computed by the $h_{B,j}$. Thus, the uncertainty in the velocity benchmark is the propagated uncertainty in the depth and flow rate benchmarks based on the formulation defined in Coleman and Steele (1995) or GUM (JCGM, 2008). When this principle is applied to the estimation of the velocity uncertainty as a function of the flow rate, depth and their respective uncertainties, the value is defined by:

$$u(V)_B = \sqrt{\left(\frac{\partial V}{\partial Q}\right)^2 u(Q)^2 + \left(\frac{\partial V}{\partial h}\right)^2 u(h)^2 + \left(\frac{\partial V}{\partial W}\right)^2 u(W)^2} \quad (4)$$

where V is the velocity in [m/s] (Eq. **3**), h is the depth in the flume in [m], w is the width of the flume channel in [m] which is a constant, and Q is the flow rate in [m^3/s]. The benchmarked velocity uncertainty, being a derived value (Aguilar et al. 2016), varies with the measured depth and EMF flow rate. As these values are not directly observable in the field application the 95% confidence interval of the velocity benchmark uncertainty was used, such that the $u(V)_B$ = 0.015 m/s.

2.4.1.2. Bias uncertainty

The bias (systematic or reducible) uncertainty is defined as the difference between the benchmarked value ($\overline{V_{B,J}}$) and the mean of i sensor observations for each trial, $(\overline{V_{EMV,J}})$. It can be calculated as the standard error of the observation residuals, which leads to the equation for Root Mean Square Error (RMSE):

$$u(V)_b = \sqrt{\frac{\sum_{i=1}^{N}\left(\overline{V_{B,J}} - \overline{V_{EMV,J}}\right)^2}{N-2}} \quad (5)$$

Following the approach introduced by the Aguilar et al. (2016), the first step was to plot the values of $\overline{V_{EMV,J}}$ against their respective benchmarked observations $\overline{V_{B,J}}$, using the line of perfect agreement (1:1 line) as a reference. Secondly, to investigate the effects of the hydraulic parameters, the measurement residuals ($\overline{V_{B,J}} - \overline{V_{EMV,J}}$) were plotted against channel depth, velocity, and Froude number Fr. Since hydraulic parameters, as well as the sediment depth, were treated as the systematic effect on the mean velocity observations, the 1:1 plots and residual plots were visually inspected for trends. Afterwards, the correction (or transformation) functions were derived for the $\overline{V_{B,J}}$ as a function of $\overline{V_{EMV,J}}$, to reduce these systematic effects. Due to the linearity of the EMV meter, linear least-

squares regression was used to create these correction functions. Correction functions were applied to the original sensor observations to remove the systematic effect of the above-mentioned parameters, thus adjusting the values towards the line of perfect agreement with benchmarked observations. The RMSE of these adjusted (corrected) results were reported as the adjusted bias uncertainty $u(V)_{b,adj}$.

By reducing the bias uncertainty, as the single reducible uncertainty component, the EMV meter was "locally calibrated" (or recalibrated) during the experiments in basic setup. Hence, in the later sediment setup and the experimental investigation with the porous sediment cover, the only systematic effect on the measurements was originating from the presence of the sediment itself.

2.4.1.3. Precision uncertainty

The random scatter of the bed mounted EMV meter observations about the mean value due to the stochasticity of the electrical and environmental conditions (i.e. aleatory uncertainty (Merz and Thieken, 2005)) is defined as the precision uncertainty ($u(V)_P$). Laboratory experiments minimize this stochasticity, although there are certain sources of non-uniformities that cannot be suppressed, such as the natural Earth magnetic variations or influence of the sensor housing on the induced turbulence. These effects are found to be acceptable as they are also met in the real field applications.

The value of the precision uncertainty was evaluated for N trials at steady state conditions, as the standard deviation of $n > 3$ mean velocity observations $S_{EMV,j}$. These standard deviation values were calculated for trials across a range of depths and velocities in the flume channel. Prior to the computation of the $u(V)_P$ visual inspection of $S_{EMV,j}$ plotted as a function of the manually observed depth, the EMF velocity, and the Froude number, needs to be performed. If no trend is present, the $u(V)_P$ can be computed as the median of all $S_{EMV,j}$, since the median is robust against non-normality and outliers.

2.4.1.4. Combined uncertainty

Finally, the combined observation uncertainty of the mean velocity is defined as the probable error range of adjusted bias, precision, and benchmark uncertainty:

$$u(V)_C = \sqrt{u(V)_{b,adj}^2 + u(V)_p^2 + u(V)_B^2} \quad (6)$$

2.4.1.5. The Uncertainty reduction factor

The calculated values for the components and the combined uncertainty of the velocity measurements were compared with the results obtained for the two ADVs, within the same price range (Aguilar et al., 2016). The relative difference between the benchmarked measurement uncertainties for the EMV and the ADV is reported through the Uncertainty Reduction Factor (URF_x), defined as the ratio of the respective uncertainty components and the combined uncertainty:

$$URF_x = \frac{u(V)_{x,ADV}}{u(V)_{x,EMV}} \quad (7)$$

where x represents one of the analyzed uncertainty components (B - benchmark, b - bias, p -precision, c - combined).

2.4.2. Assessment of the velocity sensor operation under sediment cover

Field experience has shown that sediment deposition can reduce the flow/velocity measurement accuracy, or even to stop functioning leading to the occurrence of data gaps. To allow for continuous flow measurements in UDS significant resources are needed for maintenance. However, due to the inherent integration principle of the EMV meters, these devices can be used to certain extent in the presence of porous sediment cover. To examine the capacity of velocity sensor to operate under sediment deposit a corresponding benchmarking procedure is needed. This benchmarking procedure should answer the question: How accurate mean velocity data can the particular sensor provide under a sediment deposit of specific composition and depth? As such procedure does not exist in the

literature, a novel benchmarking procedure based on the Correction Function Model (CFM), is proposed here.

The baseline assumption for novel CFM procedure is that the systematic effects on the velocity measurements (i.e. bias uncertainty) of different sediment cover depths δ_m can be reduced with the appropriate linear correction functions f_c. Each correction function f_c is defined with two parameters, slope α and intercept β. The slope α defines the amplification of the measured velocity, while the β corresponds to the zero-drift due to sediment cover. Since the benchmarks in the field application are not available, sensor observations cannot be adjusted without knowing these parameters of the correction functions. Hence, it is hypothesized that the α and β parameters of these linear functions can be accurately predicted with corresponding meta-models, $f_{amp}(\delta)$ and $f_{zero}(\delta)$, if the sediment depth δ and composition are known. Finally, it is assumed that, by defining the CFM and allowing for the measurements of the sediment depth δ at the EMV meter location, mean velocity measurements with low uncertainty can be obtained.

To test these hypothesis, 16 experimental runs with different depths δ_m of the river sand were performed as described in the section 2.3.2., on the sediment setup (section 2.3.3.). Furthermore, following procedure is proposed for the derivation of the suitable sediment specific CFM:

1.) *Uncertainty analysis.* Application of the uncertainty benchmarking analysis on each of the m-th subset data.

2.) *Correction function definition.* Linear correction functions $f_{c,m}$ derivation for the $\overline{V_{B,k,m}}$ as a function of $\overline{V_{EMV,k,m}}$, for treating the systematic effect of the sediment cover, with depth δ_m, on the velocity measurements. Each function f_m has the following form:

$$\overline{V_{B,k,m}} = \frac{\overline{V_{EMV,k,m}} - \beta_m}{\alpha_m} \tag{8}$$

where α_m [-] and β_m [m/s] are the m-th correction function slope and intercept parameter respectively.

3.) *Trend inspection*. Visual inspection of the plots: correction function parameters, slope α_m and intercept β_m, vs sediment thickness δ_m. If the trend is present, task is to define the most suitable approach for the modelling of α and β, based on the measured value of the δ_m.

4.) *Definition of the α and β parameter modelling limits.* It is excepted that due to the technology and the design of the sensor, small δ_m might not affect the sensor operation. The value of δ_m at which the sensor will start to operate with bias, defines the lower limit of the model usability. On the other hand, at high δ_m values the sensor will not produce meaningful output, hence an upper limit can be defined. Therefore, a particular set of δ_m values should be defined based on which the next step of the analysis will be performed.

5.) *Modelling of the correction function parameters α and β*. Application of the linear and non-linear regression on the $f_{c,m}$ parameters (slope α_m and intercept β_m) against the subset sediment thickness δ_m, fulfilling the criteria from step 4. The regression analysis can provide two new meta-models for the prediction of the modeled parameters: $\alpha_{m,mod} = f_{amp}(\delta_m)$ and $\beta_{m,mod} = f_{zero}(\delta_m)$. By providing these meta-models, the CFM is defined.

6.) *Validation of the CFM*. Transformation of the velocity measurements with the correction function model $f_{c,m}\left(\overline{V_{EMV,k,m}}, \alpha_{m,mod}, \beta_{m,mod}, \delta_m\right)$ and subsequent uncertainty analysis. As the uncertainty of the sediment depth measurements is $\pm$ 1 mm, the adjusted bias uncertainty of the velocity observations, corrected with the CFM, is computed as the mean of the RMSE obtained for δ_m, δ_m + 1 mm and δ_m - 1 mm.

7.) *CFM usability estimation*. Application of the uncertainty benchmarking analysis on the m-th subset data after the application of the CFM. Final estimation of the CFM usability based on the, purely empirical, two adjusted combined uncertainties criterion. This criterion is stating that the operational limit of a velocity sensor is reached when the adjusted combined uncertainty of the measurements under sediment cover is equal or larger than adjusted combined uncertainties without sediment, multiplied by two. The range of the δ at which the sensor output is unbiased define the unaffected zone (UZ). It is followed by the range of the δ fulfilling two adjusted combined uncertainties criterion, termed as the zone of the Model Applicability (MA). Values of δ above the MA are in the Out of Bounds (OoB) zone.

By applying the experimental procedure and the procedure for the definition of the CFM, the capacity of the EMV meter for operation under specific sediment cover is investigated. It should be noted that the CFM derivation is specific to both the composition of the sediment and the model of the EMV meter.

3. RESULTS AND DISCUSSION

Prior to the analysis of the collected measurements from the experimental runs, with both the basic and sediment experimental setup, the results were visually inspected. It was concluded that there were no particular issues regarding the EMV usage in the lab flume. The sensor was quickly responding to the changes in the flow, showing linear characteristics, except in the case of the formation of bed dunes. It was assumed that the high stability and repeatability of the sensor observations were primarily due to the nature of the EM velocity sensing technology.

In the following subsections, the results of the laboratory benchmarking of bias, precision, and combined uncertainty of the EMV measurements, in the basic setup, are reported and discussed. The

uncertainty of the benchmark is not analysed in details here, as it was defined in the section 2.4.1.1. Obtained results were compared with the findings reported in the research of Aguilar et al. (2016), regarding two ADV. Finally, the results of the investigation of the EMV meter performance under sediment cover is reported. CFM derivation is discussed for the river sand sediment, based on which the capacity of the EMV meter operation under sand sediment is assessed. Practical implications of the obtained results are considered, along with the framework for the field application.

3.1. Bias uncertainty

As it was discussed in section *2.4.1.2*, the reduction (adjustment) of the bias uncertainty can be interpreted as the local (re)calibration of the EMV meter. Based on the observed trends, appropriate correction (transformation) models were built to obtain the $\overline{V_{EMVadJ,J}}$ and the resulting RMSE was reported as adjusted bias uncertainty. Although the adjustment is not directly applicable to the field usage of the EMV since it compensates the local effect of the flume width, it was used for the later experiments with sediment cover.

The values of the unadjusted and adjusted bias uncertainties are reported within the **Table 1**, along with the corresponding correction function. In **Fig. 8**, the unadjusted $\overline{V_{EMV,J}}$ and adjusted $\overline{V_{EMVadJ,J}}$ values are shown against the benchmarked velocity values $\overline{V_{B,J}}$, with a referent line of for perfect agreement. The flat EMV showed good linear relationship with both unadjusted and adjusted observations (unfortunately, it was not possible to examine the linearity throughout the whole velocity range given by the manufacturer). The systematic effects from various sources can be reduced with linear correction functions, defined by only two parameters (unlike in the case of ADVs). Additionally, it supports the assumption that the slope of the original factory calibration had to be increased since the whole control volume of the sensor was not contributing to the output signal. Furthermore, this leads to the conclusion that prior to the installation of the EMV sensors in the UDS or any other hydraulic systems, a local (re)calibration procedure is needed to reduce the bias

uncertainty originating from the influence of the geometric characteristics of the flow conduit, both in terms of the velocity profiles and the control volume reach.

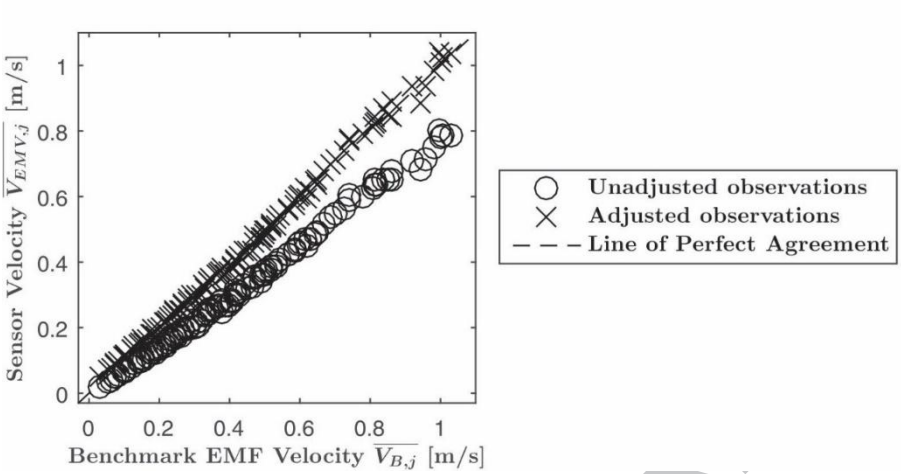

Fig. 8. Flat EMV Velocity measurements plotted against the benchmark EMF velocity with 1:1 Line of Perfect Agreement

The observed velocity residuals, before and after the correction, are plotted against the manually measured depth, benchmark (EMF) velocity, and the Froude number (**Fig. 9**). A clear relationship between the value of the residuals and the benchmarked velocity is present, which was eliminated with the appropriate correction function. The values of the residuals have a downward trend with an increase of the depth, which could be attributed to the fact that lower velocities were reported with higher depths.

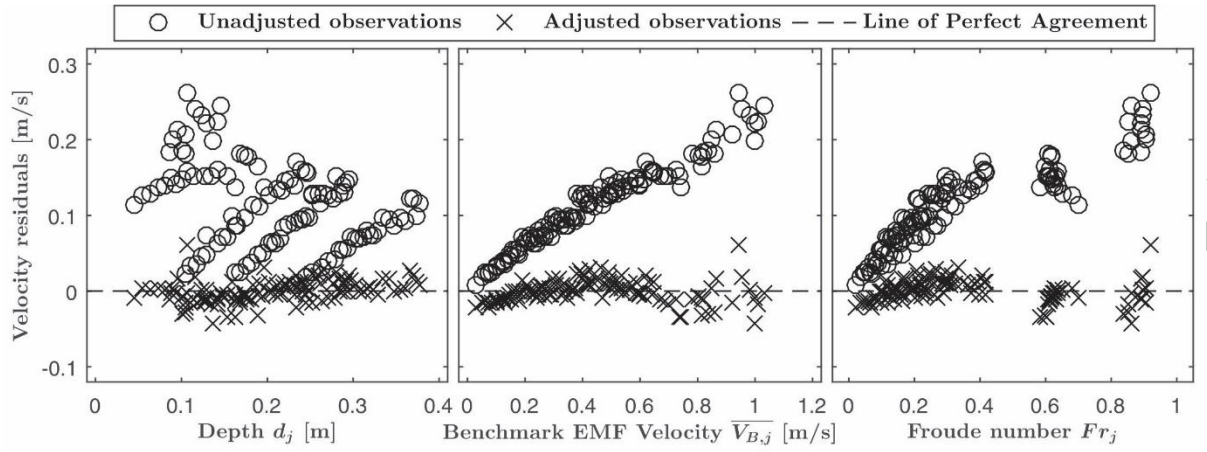

Fig. 9. EMV velocity residuals with a line of perfect agreement plotted against the manually observed depth, benchmarked velocity, and Froude number

In **Table 1**, the values of the EMV unadjusted and adjusted bias uncertainty are reported and compared with the results for two ADV sensors (Aguilar et al., 2016). The values of unadjusted bias uncertainties are not directly comparable due to the different origin (section 2.4.1.2.), therefore the focus is placed on the adjusted bias uncertainties. The value of the adjusted bias uncertainty can provide insight into the potentials of the locally calibrated EMV. It is shown that the flat EMV can operate with significantly lower bias uncertainty, with the $URF_{B,adj}$ reaching values of 3.1 and 11.5 in comparison with ADV sensors, A and B, respectively.

The presented analysis verified additional interesting aspects of the EMV usage, which could be helpful in design and management of measurement systems. Previous reviews of the ADV systems (Maheepala, 2001; McIntyre & Marshall, 2008; Aguilar et al. 2016) reported issues with the minimum detection threshold and the blanking distance, leading to erroneous measurements with low flow velocities and low flow depths. These issues were not observed in the EMV testing. **Fig. 9**. shows that the flat EMV was capable of accurately measuring the velocity with the low depth, as low as 4 cm (~2 cm of distance between the electrodes and the water surface). Furthermore, velocities as low as 3 cm/s were measured, which can be particularly useful in the case of the flow measurements in conduits with shallow gradient and/or under (pluvial) backwater effect.

Table 1.

Comparison between the results of the uncertainty benchmarking procedures between the flat EMV and two ADVs (Aguilar et al., 2016)

Sensor	Type	Number of trials	Correction function	Unadjusted Bias Uncertainty * [m/s]	Adjusted Bias Uncertainty [m/s]	Precision Uncertainty [m/s]	Bench Uncer [m/s]
1	flat EMV	114	$(V - 0.020)/0.790$	0.128	0.015	0.006	0.015
2	ADV	287	$0.875 \cdot V^{0.968}$	0.096	0.048	0.015	0.017
3	ADV	349	$0.692 \cdot V^{0.912}$	0.439	0.179	0.067	0.017
Uncertainty reduction factors			$URF_{x,A}$	0.75	3.13	2.41	1.13
			$URF_{x,B}$	3.43	11.57	10.63	1.13

* Comparison is not valid due to the different origin of the uncertainty

3.2. Precision uncertainty

The precision uncertainty of the EMV was defined as the standard deviation of $n > 3$ observations ($S_{V,EMV,j}$), when the flow conditions in the flume were at steady state. Results were examined for trends between the standard deviation and manually observed depth, benchmarked velocity and Froude number (**Fig. 10**). It can be seen from the **Fig. 10**, that there is no significant correlation between the standard deviation and the examined parameters, except in the comparison with the EMF velocity. This slightly increasing trend could originate from the non-streamlined design of the housing, although it should be verified with further experiments. It is expected that with the increased

velocity, the coherent turbulent structures near the edges of the housing start to influence the measurements. However, the values of the standard deviation are still lower than values reported for the ADV sensors. The URF_p achieved in the comparison with the ADV A and B, is 2.4 and 10.6, respectively (**Table 1**).

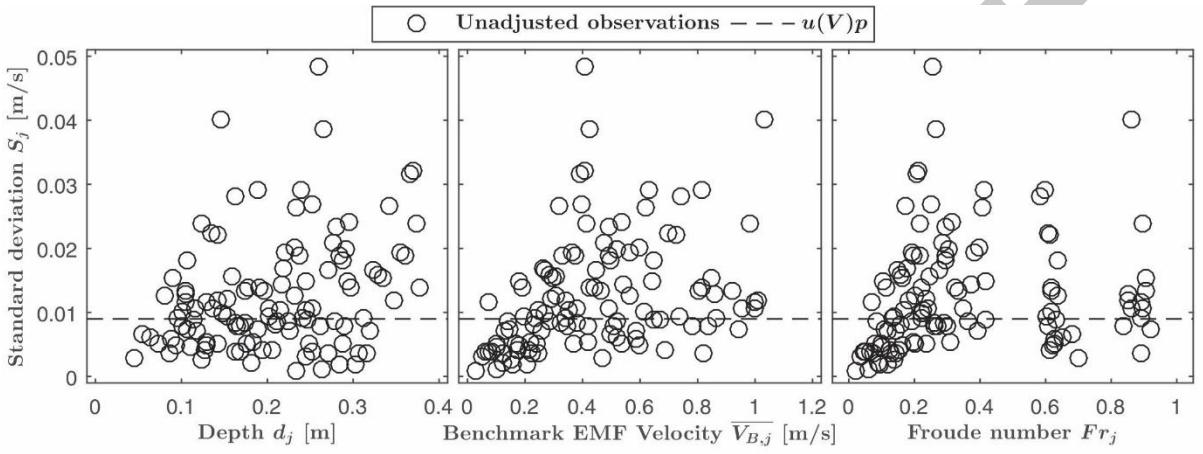

Fig. 10. EMV standard deviation with the precision uncertainty plotted against the manually observed depth, benchmarked velocity and Froude number

3.3 Combined uncertainty

The contributions from all the uncertainty components (bias, precision, and benchmark) are aggregated into the value of the combined uncertainty. **Table 1** shows that the URF_c for the combined uncertainty are 2.4 or 8.5 in comparison to the ADV sensors A and B, respectively. The presented reduction in the observational uncertainty should be primarily attributed to the EM velocity sensing technology. The results were somewhat expected, as this technology has a clear physical integrative background, which allows for the stable and robust velocity measurements.

3.4 Assessment of the velocity sensor operation under sediment cover

Following the procedure proposed in the section 2.4.2., measurements necessary for benchmarking observational uncertainty were conducted with 16 different sediment depths δ_m. The CFM was defined and validated within the followingsteps:

1.) *Uncertainty analysis.* Analysis for benchmarking measurement uncertainty, presented in section 2.3. was applied on the locally calibrated EMV meter measurements, on each of the m-th subset data. The results are presented on the **Fig. 11.**

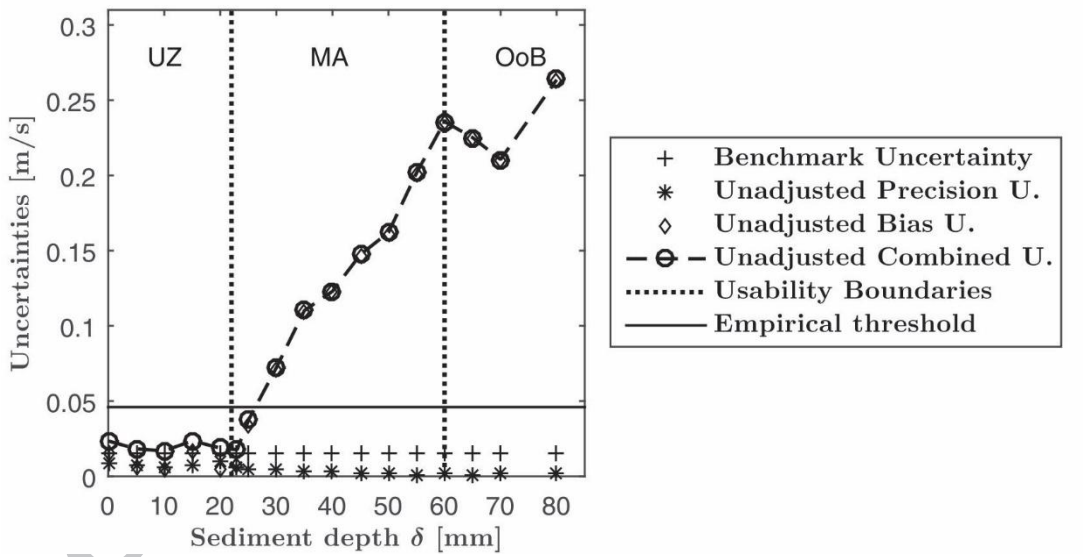

Fig. 11. Benchmark and adjusted precision, bias and combined uncertainties against sand sediment depths

2.) *Correction function definition.* It can be observed that the bias uncertainty increases with the rise of the sediment depth δ_m. These results confirmed the theory described in the section 2.1.2., that by excluding the zones close to the sensor, the effective control volume of the EMV meter gets smaller and moves further from the sensor where magnetic field is weaker, resulting with exponentially smaller output signal. To reduce the resulting bias uncertainty

linear correction functions $f_{c,m}$ are derived, defined by two parameters α_m and β_m, while those two parameters are nonlinear function of sediment depth (see next step).

3.) *Trend inspection*. Parameters α_m and β_m were plotted against sediment depth δ_m, **Fig. 12** and **13** respectively. It was concluded that the slope parameter (i.e. output amplification) has a clear power-like correlation with the δ_m (**Fig. 12**), while β_m (i.e. zero velocity drift, or offset drift) is relatively small and varies around two constant values with the jump in between (**Fig. 13**).

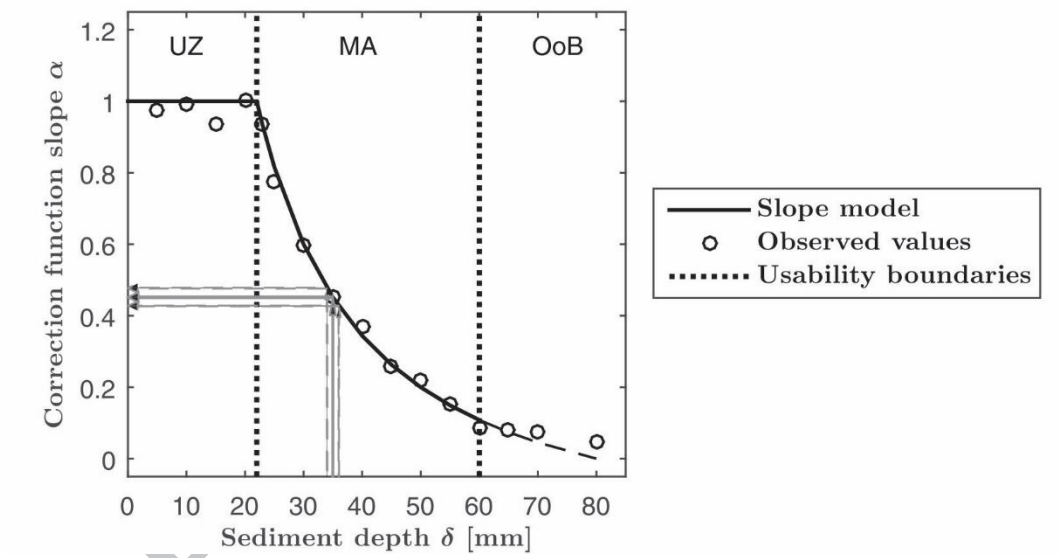

Fig. 12. Correction function slope α_m against the sediment depth with corresponding power model

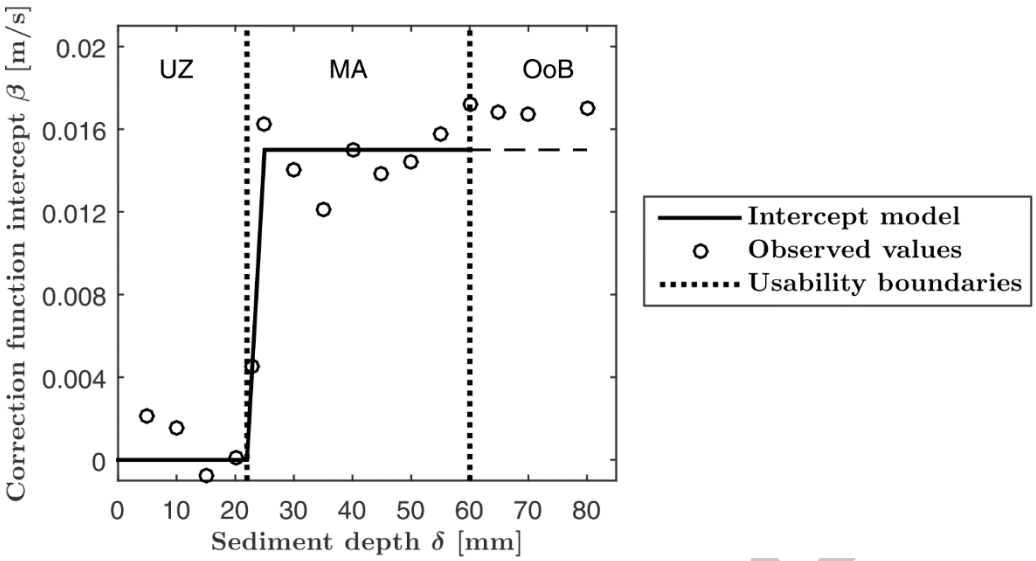

Fig. 13. Correction function intercept β_m against the sediment depth with corresponding compound linear model

4.) *Definition of the α and β parameter modelling limits.* Based on the visual comparison of the **Fig. 11 - 13**, it was realized that, at the sediment depth of δ_m = H = 23 mm, the presence of the sediment starts to affect the velocity measurements. Since the probe height without electrodes is 22 mm and the electrodes height is 1 mm, the physical based lower limit of the CFM model application was chosen to be equal to H-1 mm = 22 mm (the lower 'Usability boundary' on the Fig.14). Additionally, it was observed that for the sediment depths higher than δ_m = 60 mm, the EMV meter produces very small output. Hence the upper limit of the CFM model application was assumed to be around 60 mm.

5.) *Modelling of the correction function parameters α and β*. The α parameter was modelled using the non-linear regression for the range of δ_m between 22 and 60 mm (**Fig. 12**). For the same range of δ_m, model for parameter β was proposed with steep linear jump between δ_m= 22 and 25 mm and the constant value for δ_m= 25 - 60 mm (**Fig. 13**). Hence the CFM model for the examined EMV meter and sand sediment was derived.

6.) *Validation of the CFM*. Locally calibrated velocity measurements $\overline{V_{EMV,k,m}}$, for each of the m-th subset data, were corrected with the CFM model (f_c, $f_{amp}(\delta_m)$ and $f_{zero}(\delta_m)$). Hence, for each of the examined δ_m, the parameters of the corresponding correction functions were predicted, $\alpha_{m,mod}\left(f_{amp}(\delta_m)\right)$ and $\beta_{m,mod}\left(f_{zero}(\delta_m)\right)$. Measurements prior to the adjustment with the CFM, along with the lines of the perfect agreement, are plotted on **Fig. 14**. Uncertainty bounds illustrate the propagation of the uncertainty in the sediment height measurements and show the effect on the correction function parameters for δ_m ± 1 mm. The results corresponding to the benchmarked velocities higher than 0.3 m/s were excluded as they were biased by uncontrollable bed dunes formation, except in the additional experiment with δ_m = 23 mm (surface of the electrodes - H). Here, smaller fractions formed the thin sediment cover between the surface of the electrodes and the sensor's housing upper surface (~ 22 mm). Hence the sediment movement started with lower mean velocity contributing to the earlier loss of the EMV's linearity property (**Fig. 6 B**).

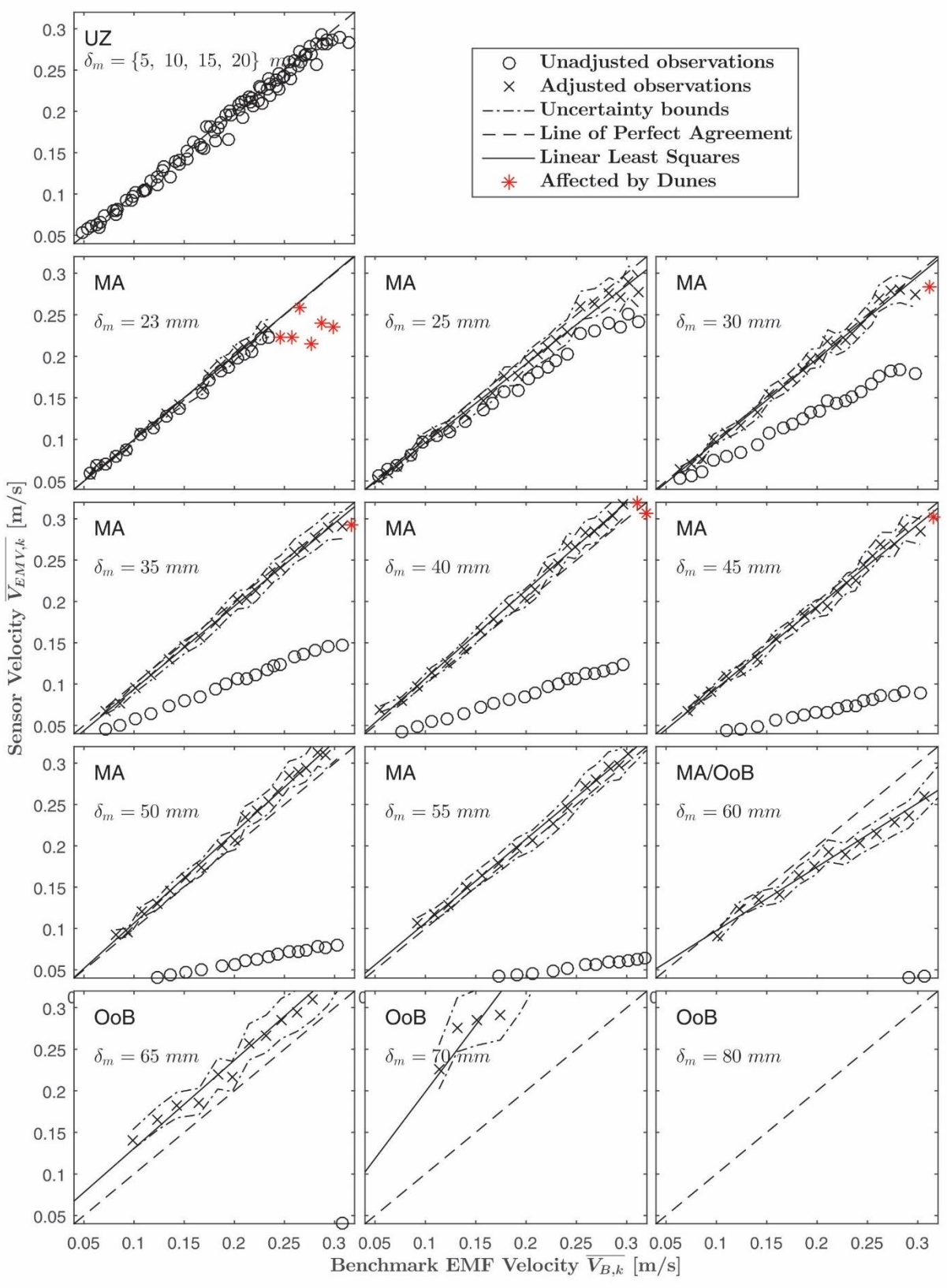

Fig. 14. EMV velocity observations $\overline{V_{EMV,k,m}}$ prior and after the application of the presented correction function model for the operation under sand sediment deposit

7.) *CFM usability estimation*. After performing subsequent uncertainty analysis on the measurements corrected with the CFM, usability of the CFM model was estimated (**Fig. 15**). Empirical criterion, based on the value of two adjusted combined uncertainties, was used (represented with the black horizontal line on **Fig. 11** and **Fig. 15**).

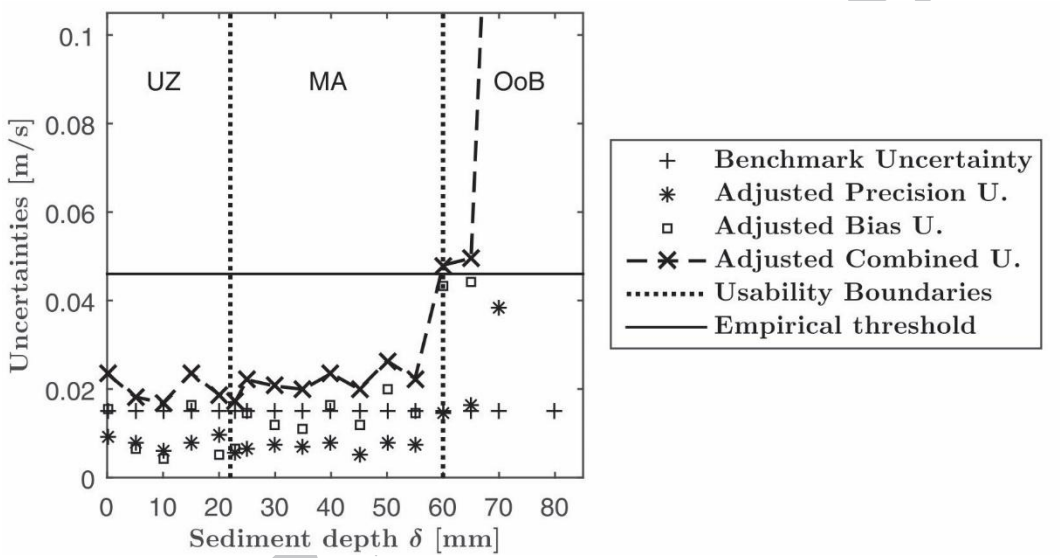

Fig. 15. Benchmark and unadjusted precision, bias and combined uncertainties against sand sediment depths

First the Unaffected Zone (UZ) is defined for the range of sand sediment depths $\delta_m = 0 - 22$ mm (**Fig. 11 – 15)**. In this zone the flat EMV meter can operate without the need for the measurement corrections. The measurements within the UZ were grouped on a single plot in the upper left corner of the **Fig. 14**. The range of $\delta_m = 22 - 60$ mm defines the zone for the correction function model applicability (MA), where it is expected that the EMV can provide accurate velocity measurements, if the sediment depth is measured and CFM is applied. It can be seen on **Fig. 14** that for MA zone and within the specified mean velocity range (up to the 0.3 m/s), the corrected velocity observations show a good agreement with the benchmarked

values. At the boundary between the MA and OoB zone, for the δ_m = 60 mm, the agreement is starting to vanish as the adjusted combined uncertainty shows exponential growth (**Fig. 15**). Finally, values of δ_m above 60 mm are Out of Bounds (OoB) of the model, and it is assumed that here, velocity measurements cannot be corrected in valid manner.

Furthermore, the physical meaning of the $f_{amp}(\delta_m)$ and $f_{zero}(\delta_m)$ models was considered. It is suspected that the non-linear correlation between α_m and δ_m, within MA zone, is stemming from the EMV's non-linear weighting function. Thus, the gradient of the amplification values α_m is highest at the beginning of the MA zone – where the magnetic field $\vec{B}$ and virtual current $\vec{j}$ (Eq. **2**) have maximum values; and is decreasing along with the $\vec{B}$ and $\vec{j}$. However, the zero-drift parameter β_m seems to be affected only by the presence of the sand sediment on the electrode's surface (it effectively reduces the electrode size) as it was relatively constant for higher δ_m values.

3.5 Practical implications

The presented analysis had two goals: firstly, the analysis of the performance of the EMV meter in regular lab conditions was considered, providing an unbiased comparison with the ADV; secondly the prospect of the EMV usage under the porous sediment cover was investigated and novel benchmarking procedure was developed for the quantification of the operational limits. Practical implications of the findings remain to be verified in the field but presented experimental results are sufficient support for the hypothesis that the EMV meters can provide additional value in the flow monitoring in the UDS. Several benefits of the EMV usage have been verified in this research and are highlighted:

- The first significant benefit is the possibility of EMV to operate in low flow depths (4 cm) and low flow velocities (3 cm/s), which is clearly supported by the results in **Table 1** and **Fig.**

8-10. Thus, the EMV meter can cover a wider range of hydraulic conditions than the ADV, which can be particularly useful in combined sewer systems.

- The second important feature of the EMV is the linearity in the examined velocity range. This property allows for the reduction of the systematic effects with the simple linear correction functions defined by amplification and zero-drift parameter (**Table 1** and Eq. **8**).

- Furthermore, the uncertainty benchmarking procedure revealed that the EMV devices are superior over ADVs, in terms of the stability and repeatability. This is verified with the value of the Uncertainty Reduction Factor $URF_p > 2.4$, even though shorter measurement time intervals were used (section 2.3.1.).

- If the pre-positioning/local (re)calibration procedure is performed prior to the measurements, EMV meters can also be more accurate than ADVs ($URF_c > 2.3$).

- The most significant characteristic of the EMV is its capacity for the velocity monitoring under the porous sediment cover, with the use of the presented CFM. In practice, however, some additional considerations should be taken into account when designing flow measuring site equipped with the EMV for UDS. Firstly, the composition of the local-specific sediment must be investigated prior to the installation of the EMV. If possible, a proposed benchmarking procedure, with local sediment, should be conducted for the formulation of the appropriate CFM. Although the results from this work might be helpful, they can also be misleading due to the reported heterogeneity of the sediments sampled from different locations (Crabtree, 1989; Skipworth et al., 1999). As the sediment deposition is time dependent, accurate real-time assessment of the sediment thickness δ, around or above the EMV, must be provided. Recent advances in the acoustic measurements of sediments in

sewers (Lepot et al., 2017), show promising results with the reported uncertainties being only 4%.

All the listed benefits are attributed to the very nature of the EM velocity sensing technology. However, the biggest downside of the EMV meters is limited control volume, in comparison with the ADV. It is difficult to circumvent this unwanted property of the EM technology; therefore, it presents an important constraint in the EMV meter usage. As the problem with the control volume representativeness is common for the velocity-area methods (Bonakdari & Zinatizadeh, 2011), additional care is needed when positioning an EMV device inside the flow conduit. Therefore, a sort of the pre-positioning analysis is needed for the definition of the optimal position of the sensor. Thus, additional resources are needed for the appropriate application of the EMV in hydraulic systems.

4. CONCLUSIONS

The results of the laboratory benchmarked uncertainties in velocity measurements obtained for the flat EMV meter support the idea of the application of this technology for flow measurement in UDS. This can be considered either as an alternative or, even a supplement to ADV where best of two technologies could be put to work together. The usage of the experimental setup and procedure similar to the one employed in previous investigations, allowed a direct comparison of the two methods. When compared to the benchmarked values given by Aguilar et al. (2016) for the two models of the ADV, it was shown that flat EMV meter provides more accurate and precise velocity measurements in the laboratory conditions. Furthermore, it was concluded that due to the nature of the EM velocity sensing technology, EMV can accurately characterize velocities in the broader range of hydraulic conditions.

The flat EMV capability of operation under porous sediment deposit was investigated using the novel laboratory benchmarking procedure. The procedure included experiments of sensor operation under

sediment deposits with varying depths. River sand was used to model the influence of porous sediment deposit, usually found in storm and combined sewers. It was shown that deposits higher than 22 mm cause a systematic influence on the EMV meter's characteristics. Consequently, an appropriate Correction Function Model (CFM) was derived to compensate for that systematic effect. The slope and intercept parameters of each correction function (for each sediment depth) obtained through a linear least-square regression, were modelled as a functions of sediment depth. The linear correction function with non-linear parameter model formulate a CFM which allows for the velocity measurements to be corrected based only on the sediment depth. The uncertainty analysis of these adjusted mean velocity measurements showed that this approach has a potential to improve the practical application. The resulting adjusted combined uncertainties for the sand sediment depths up to 60 mm were in the range of the uncertainties reported for the sensor application without the sediment cover. However, the analysis revealed that the correction function model can be applied only in the case of the flat sediment surface. With the increase of the mean flow velocities over 0.3 m/s, bed dunes were formed in the sand sediment diminishing the linearity property of the EMV. Therefore, it is necessary to determine the relationship between the bed dune dimensions and the bias uncertainty of the velocity observations made with the EMV.

Although EMV technology has proven to have interesting advantages for the application in UDS, it is constrained by a significant drawback: the measuring control volume of the bed-mounted flat EMV is relatively close to the probe and significantly smaller than those of the typical bed-mounted ADV. Thus, it is recommended that prior to the installation, a pre-positioning analysis is performed to select the optimal size (larger EMV probes will have larger control volume) and position of the sensor (probe can be installed to penetrate in cross section, or several probes could be combined). Furthermore, this analysis should also include the local (re)calibration of the EMV meter, in order to compensate the systematic effects on the velocity measurements.

The analysis presented within this paper was limited to assessment of the operational characteristics of the flat EMV in the laboratory conditions with and without static sediment deposit. Further field investigations should quantify the additional sediment related impacts, like mobile bed and floating

debris. Additionally, EMV operation under more site-specific sediment cover is needed, as classified in the research of Crabtree (1989). Finally, a derivation of the robust pre-positioning analysis is required, probably supported by CFD analysis, which will allow practitioners to better locally (re)calibrate the EMV and hence exploit the benefits of its usage in UDS. The results of suggested research should lead to the development of a robust operational framework for improving the accuracy of the continuous discharge measurements in UDS.

ACKNOWLEDGEMENTS

The authors express the gratitude to the Serbian Ministry of Education and Science for the support through the project TR37010: "Rain water drainage systems as part of the urban and transport infrastructure".

REFERENCES

1. Aguilar, M.F. and Dymond, R.L., 2014. Innovative technologies for storm-water management programs in small urbanized areas. *Journal of Water Resources Planning and Management*, 140(11), p.04014029.
2. Aguilar, M.F., McDonald, W.M. and Dymond, R.L., 2016. Benchmarking laboratory observation uncertainty for in-pipe storm sewer discharge measurements. *Journal of Hydrology*, 534, pp.73-86.
3. Ashley, R.M., Bertrand-Krajewski, J.L., Hvitved-Jacobsen, T. and Verbanck, M. eds., 2004. *Solids in sewers*. IWA Publishing.
4. Banasiak, R., 2008. Hydraulic performance of sewer pipes with deposited sediments. *Water Science and Technology*, 57(11), pp.1743-1748.

5. Bertrand-Krajewski, J.L., Bardin, J.P., Mourad, M. and Beranger, Y., 2003. Accounting for sensor calibration, concentration heterogeneity, measurement and sampling uncertainties in monitoring urban drainage systems. *Water Science and Technology*, 47(2), pp.95-102.
6. Bertrand-Krajewski, J.L. and Muste, M., 2008. Understanding and managing uncertainty. *Data requirements for integrated urban water management*. Edited by: Tim Fletcher and Ana Deleti? (Vol. 1). Paris: UNESCO Publishing and Taylor & Francis.
7. Bevir, M.K., 1970. The theory of induced voltage electromagnetic flowmeters. *Journal of Fluid Mechanics*, 43(3), pp.577-590.
8. Bevir, M.K., O'sullivan, V.T. and Wyatt, D.G., 1981. Computation of electromagnetic flowmeter characteristics from magnetic field data. *Journal of Physics D: Applied Physics*, 14(3), p.373.
9. Bonakdari, H. and Zinatizadeh, A.A., 2011. Influence of position and type of Doppler flow meters on flow-rate measurement in sewers using computational fluid dynamic. *Flow Measurement and Instrumentation*, 22(3), pp.225-234.
10. Butler, D., May, R. and Ackers, J., 2003. Self-cleansing sewer design based on sediment transport principles. *Journal of Hydraulic Engineering*. 129(12), 276-282.
11. Campisano, A., Cabot Ple, J., Muschalla, D., Pleau, M. and Vanrolleghem, P.A., 2013. Potential and limitations of modern equipment for real time control of urban wastewater systems. *Urban Water Journal*, 10(5), pp.300-311.
12. Coleman, H.W. and Steele, W.G., 1995. Engineering application of experimental uncertainty analysis. *AIAA journal*, 33(10), pp.1888-1896.
13. Crabtree, R.W., 1989. Sediments in sewers. *Water and Environment Journal*, 3(6), pp.569-578.
14. Gils, H., 1970. Discharge measurement in open water by means of magnetic induction. *In Symposium on hydrometry*, Koblenz.
15. Godley, A., 2002. Flow measurement in partially filled closed conduits. *Flow Measurement and Instrumentation*, 13(5), pp.197-201.

16. Harremoës, P., Capodaglio, A.G., Hellström, B.G., Henze, M., Jensen, K.N., Lynggaard-Jensen, A., Otterpohl, R. and Søeberg, H., 1993. Wastewater treatment plants under transient loading-Performance, modelling and control. *Water Science and Technology*, 27(12), p.71.
17. Heiner, B.J. and Vermeyen, T.B., 2012. Laboratory evaluation of open channel area-velocity meters. US Bureau of Reclamation, Denver, CO, p.15.
18. Herschy, R.W. and Newman, J.D., 1974. Electromagnetic River Gauging, symposium on river gauging by electromagnetic methods. Water Research Centre and Department of the Environment.
19. Herschy, R.W., 1978. Accuracy in Hydrometry. Wiley, New York.
20. ISO9104, 1991. Measurement of fluid flow in closed conduits-Methods of evaluating the performance of electromagnetic flow-meters for liquids, International Organization for Standardization.
21. Joint committee for Guides in Metrology (JCGM), 2008. Guide to the expression of uncertainty in measurement. International Organization for Standardization.
22. Kolin, A., 1936. An electromagnetic flowmeter. Principle of the method and its application to bloodflow measurements. *Proceedings of the Society for Experimental Biology and Medicine*, 35(1), pp.53-56.
23. Kuromori, K., Gotoh, S. and Matunaga, Y., 1994. An electromagnetic flowmeter with dual frequency excitation. *Transactions of the Society of Instrument and Control Engineers*, 30(9), pp.1020-1026.
24. Larrarte, F., Bardiaux, J.B., Battaglia, P. and Joannis, C., 2008. Acoustic Doppler flow-meters: A proposal to characterize their technical parameters. *Flow Measurement and Instrumentation*, 19(5), pp.261-267.
25. Leeungculsatien, T. and Lucas, G.P., 2013. Measurement of velocity profiles in multiphase flow using a multi-electrode electromagnetic flow meter. *Flow Measurement and Instrumentation*, 31, pp.86-95.

26. Lepot, M., Pouzol, T., Aldea Borruel, X., Suner, D. and Bertrand-Krajewski, J.L., 2017. Measurement of sewer sediments with acoustic technology: from laboratory to field experiments. *Urban Water Journal*, 14(4), pp.369-377.

27. Maheepala, U.K., Takyi, A.K. and Perera, B.J.C., 2001. Hydrological data monitoring for urban stormwater drainage systems. *Journal of Hydrology*, 245(1-4), pp.32-47.

28. McIntyre, N. and Marshall, M., 2008, August. Field verification of bed-mounted ADV meters. *In Proceedings of the Institution of Civil Engineers-Water Management* (Vol. 161, No. 4, pp. 199-206). ICE Publishing.

29. McMillan, H., Krueger, T. and Freer, J., 2012. Benchmarking observational uncertainties for hydrology: rainfall, river discharge and water quality. *Hydrological Processes*, 26(26), pp.4078-4111.

30. Merz, B. and Thieken, A.H., 2005. Separating natural and epistemic uncertainty in flood frequency analysis. *Journal of Hydrology*, 309(1-4), pp.114-132.

31. Michalski, A., Starzynski, J. and Wincenciak, S., 2001. Electromagnetic flowmeters for open channels: two-dimensional approach to design procedures. *IEEE sensors journal*, 1(1), pp.52-61.

32. Michalski, A., Starzynski, J. and Wincenciak, S., 2002. 3-D approach to designing the excitation coil of an electromagnetic flowmeter. *IEEE Transactions on Instrumentation and measurement*, 51(4), pp.833-839.

33. Moffat, R.J., 1988. Describing the uncertainties in experimental results. *Experimental thermal and fluid science*, 1(1), pp.3-17.

34. Nord, G., Gallart, F., Gratiot, N., Soler, M., Reid, I., Vachtman, D., Latron, J., Martín-Vide, J.P. and Laronne, J.B., 2014. Applicability of acoustic Doppler devices for flow velocity measurements and discharge estimation in flows with sediment transport. *Journal of hydrology*, 509, pp.504-518.

35. Nortek, A.S., 2009. Vectrino velocimeter user guide. *Nortek AS, Vangkroken, Norway*, *621*.

36. Owen, H.J., 1979. Information for Local Officials on Flood Warning Systems. National Weather Servic, Palo Alto, California. Retrieved from http://hdl.handle.net/2027/uc1.31822017076480.

37. Prodanović, D., 2008. Selecting monitoring equipment. *Data Requirements for Integrated Urban Water Management*. Edited by: Tim Fletcher and Ana Deletić (Vol. 1). Paris: UNESCO Publishing and Taylor & Francis.

38. Prodanović, D., Djačić, A., Branisavljević, N. and Rukavina J., 2012. Laboratory tests of ultrasound and electromagnetic devices for flow measurements in sewer systems. *Current issues in water supply and sewage 2012*, Bol on Brač (In Serbian/Croatian language).

39. Roy, A.H., Wenger, S.J., Fletcher, T.D., Walsh, C.J., Ladson, A.R., Shuster, W.D., Thurston, H.W. and Brown, R.R., 2008. Impediments and solutions to sustainable, watershed-scale urban stormwater management: lessons from Australia and the United States. *Environmental management*, 42(2), pp.344-359.

40. Schütze, M., Butler, D., Beck, M.B. and Verworn, H.R., 2002. Criteria for assessment of the operational potential of the urban wastewater system. *Water science and technology*, 45(3), pp.141-148.

41. Schütze, M., Campisano, A., Colas, H., Schilling, W. and Vanrolleghem, P.A., 2004. Real time control of urban wastewater systems-where do we stand today? *Journal of hydrology*, 299(3-4), pp.335-348.

42. Shercliff, J.A., 1962. The theory of electromagnetic flow-measurement. CUP Archive.

43. Skipworth, P.J., Tait, S.J. and Saul, A.J., 1999. Erosion of sediment beds in sewers: Model development. *Journal of environmental engineering*, 125(6), pp.566-573.

44. Steinbock, J., Weissenbrunner, A., Juling, M., Lederer, T. and Thamsen, P.U., 2016. Uncertainty evaluation for velocity-area methods. *Flow Measurement and Instrumentation*, 48, pp.51-56.

45. Svet instrumenata, 2018. Flat DC2.34 EMV. Product Datasheet (In Serbian). Retrieved from < http://www.si.co.rs/index-e.html >.

46. Watral, Z., Jakubowski, J. and Michalski, A., 2015. Electromagnetic flow meters for open channels: Current state and development prospects. *Flow measurement and Instrumentation*, 42, pp.16-25.

47. WERF, 2002. Assess and Document Installed State-of-the-Art WWTP Sensing and Control Systems. Draft Report, Project 99-WWF-4. Alexandria, Virginia: WERF.

Table 1.

Comparison between the results of the uncertainty benchmarking procedures between the flat EMV and two ADVs (Aguilar et al., 2016)

Sensor	Type	Number of trials	Correction function	Unadjusted Bias Uncertainty * [m/s]	Adjusted Bias Uncertainty [m/s]	Precision Uncertainty [m/s]	Bench Uncer [m/s]
1	flat EMV	114	$(V - 0.020)/0.790$	0.128	0.015	0.006	0.015
2	ADV	287	$0.875 \cdot V^{0.968}$	0.096	0.048	0.015	0.017
3	ADV	349	$0.692 \cdot V^{0.912}$	0.439	0.179	0.067	0.017
Uncertainty reduction factors			$URF_{x,A}$	0.75	3.13	2.41	1.13
			$URF_{x,B}$	3.43	11.57	10.63	1.13

* Comparison is not valid due to the different origin of the uncertainty

Highlights

- Bed-mounted EMV meters can operate in a wide range of hydraulic conditions.
- EMV meters have higher stability and repeatability than the ADVs.
- EMV meters are linear in a wide range of velocities.
- EMV meters can provide accurate velocity measurements under porous sediment cover, if the sediment depth is known.